

# Stratospheric gas variations: Comparing ACE and MKIV balloon

Geoff Toon

Jet Propulsion Laboratory

California Institute of Technology

2024-10-08



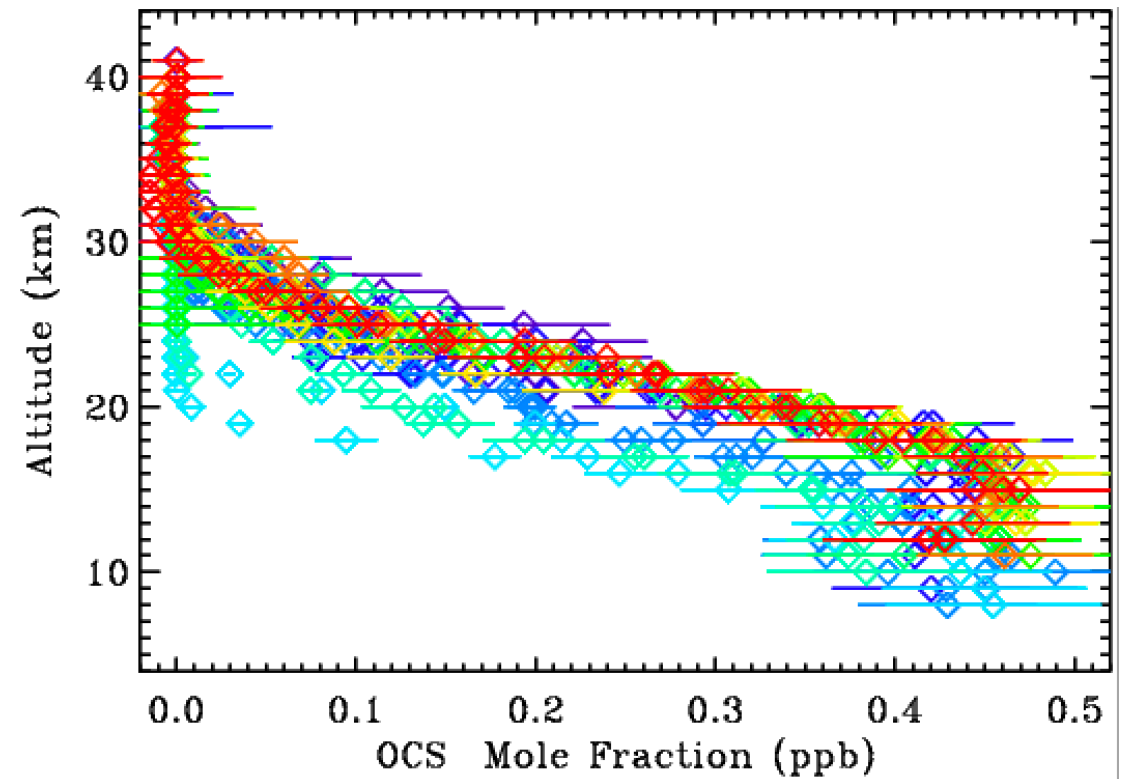
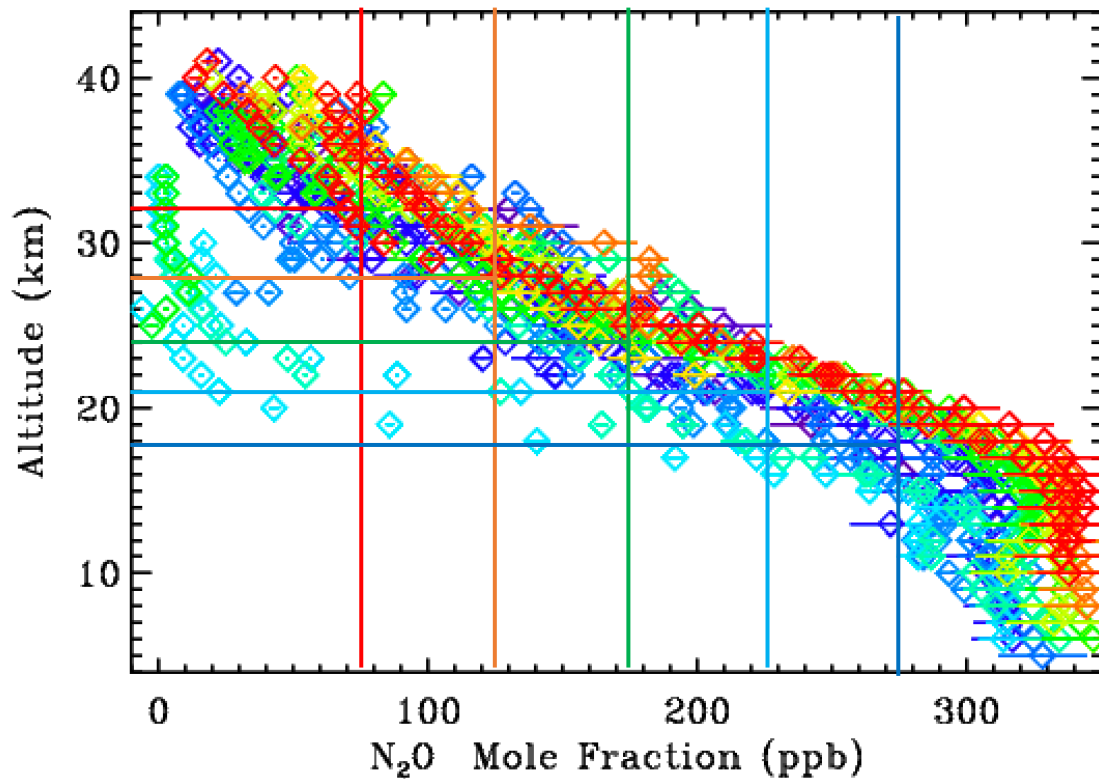
The MKIV interferometer is a solar occultation FTS covering the 650-5650  $\text{cm}^{-1}$  range at 0.01  $\text{cm}^{-1}$  resolution (56 cm MOPD) for balloon flights. It has performed 28 balloon flights (mostly from 35N), ground-based observations, and has previously flown 3 campaigns on NASA DC-8 aircraft. No close co-incidences with ACE: late Sep at 35N falls in a hole in ACE coverage.

MKIV averages only 1 occultation per year. So using MKIV data for trend assessment is difficult, because even for balloon flights launched from the same site and month, the origin of the probed airmasses varies from flight to flight due to stratospheric transport differences. One year the the MKIV may be sampling sub-tropical airmasses, whereas the next year, from the exact same location and date, it might sample mid-latitude airmasses.

Using a tracer  $\text{N}_2\text{O}$  as a vertical ordinate helps remove some of this dynamical variability, allowing the underlying trends to be more clearly seen.



## Example: MkIV profiles of N<sub>2</sub>O and OCS versus altitude



Profiles of N<sub>2</sub>O (left) and OCS (right) color-coded by year (blue = 1989; green = 2004; red = 2021, etc.). OCS is shorter lived and therefore decreases more rapidly with altitude, but there is a similarity in the behavior of the N<sub>2</sub>O and OCS profiles.

Profiles are variable from flight to flight. High latitude flights (cyan, green) have less gas at a given altitude due to downward transport at high latitudes. But even among the mid-latitude flights, there is still a lot of variation. So, when we try to estimate the trends at altitudes of 19, 22, 24, 27, and 32 km, the results look very noisy (next slide)

Plotting versus altitude above the tropopause or potential temperature (not shown) reduces scatter, but not by much.

# Compact relationship between N<sub>2</sub>O and OCS

Measured OCS and N<sub>2</sub>O mole fractions plotted against each other, color-coded by year (purple=1989, blue=1992, green=2004; red=2023).

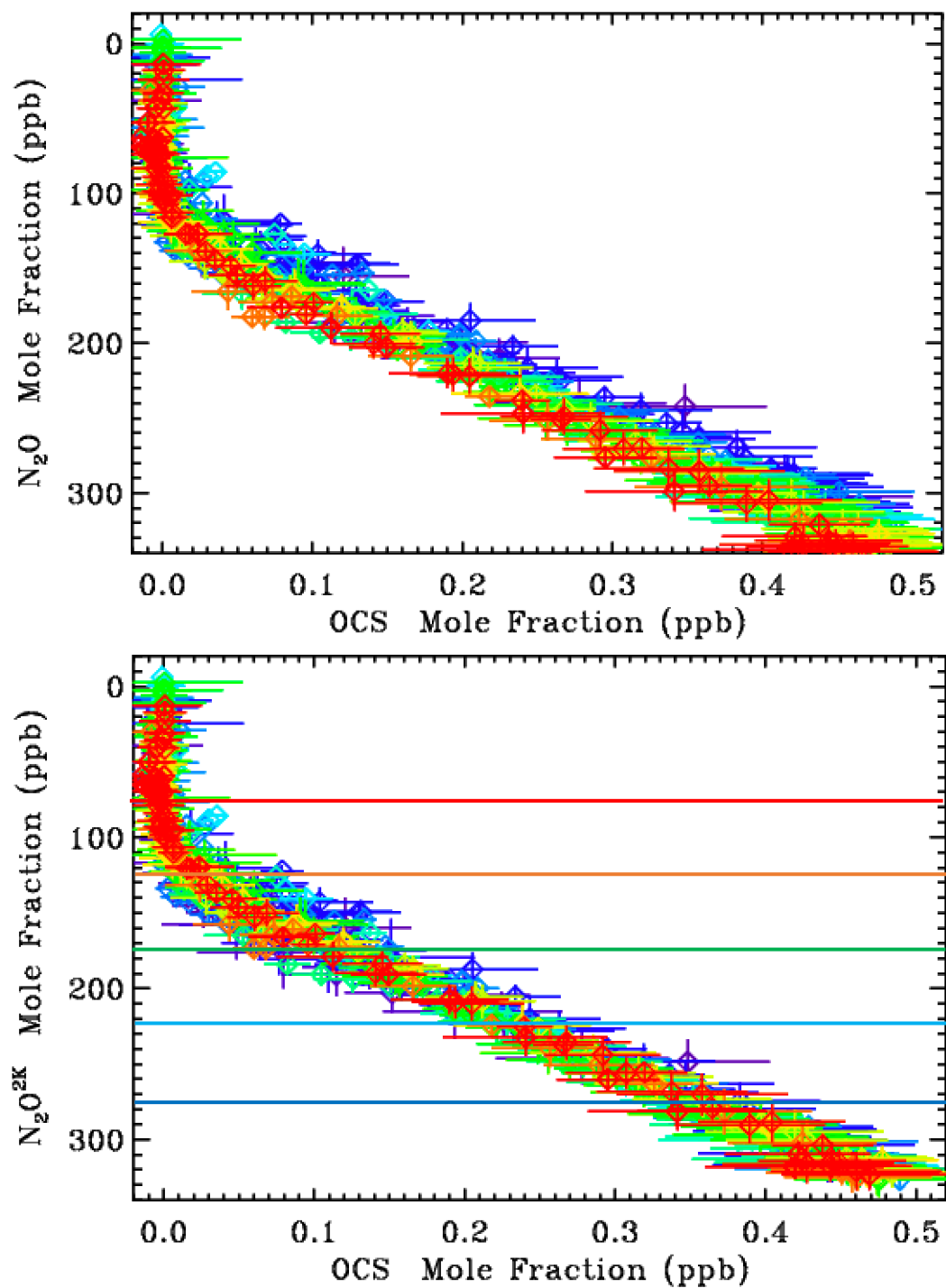
Top panel showing raw data shows a creeping increase of N<sub>2</sub>O or decrease of OCS over time. Since we know from other measurements (e.g. in situ and ACE) that N<sub>2</sub>O has been increasing by 0.26% per year over the past 30 years, we can correct the measured N<sub>2</sub>O values back to the value that they would have been in 2000 using the equation

$$N_2O^{2K} = N_2O / [1 + 0.0026 * (\text{year} - 2000)]$$

The lower panel shows the OCS plotted versus N<sub>2</sub>O<sup>2K</sup>. There is no obvious creep over time since all the different colors lie on the same compact relationship. This implies little or no OCS trend.

We can now look for trends on the five isopleths: N<sub>2</sub>O<sup>2K</sup> = 75, 125, 175, 225, 275 ppb, denoted by the colored horizontal lines in lower panel.

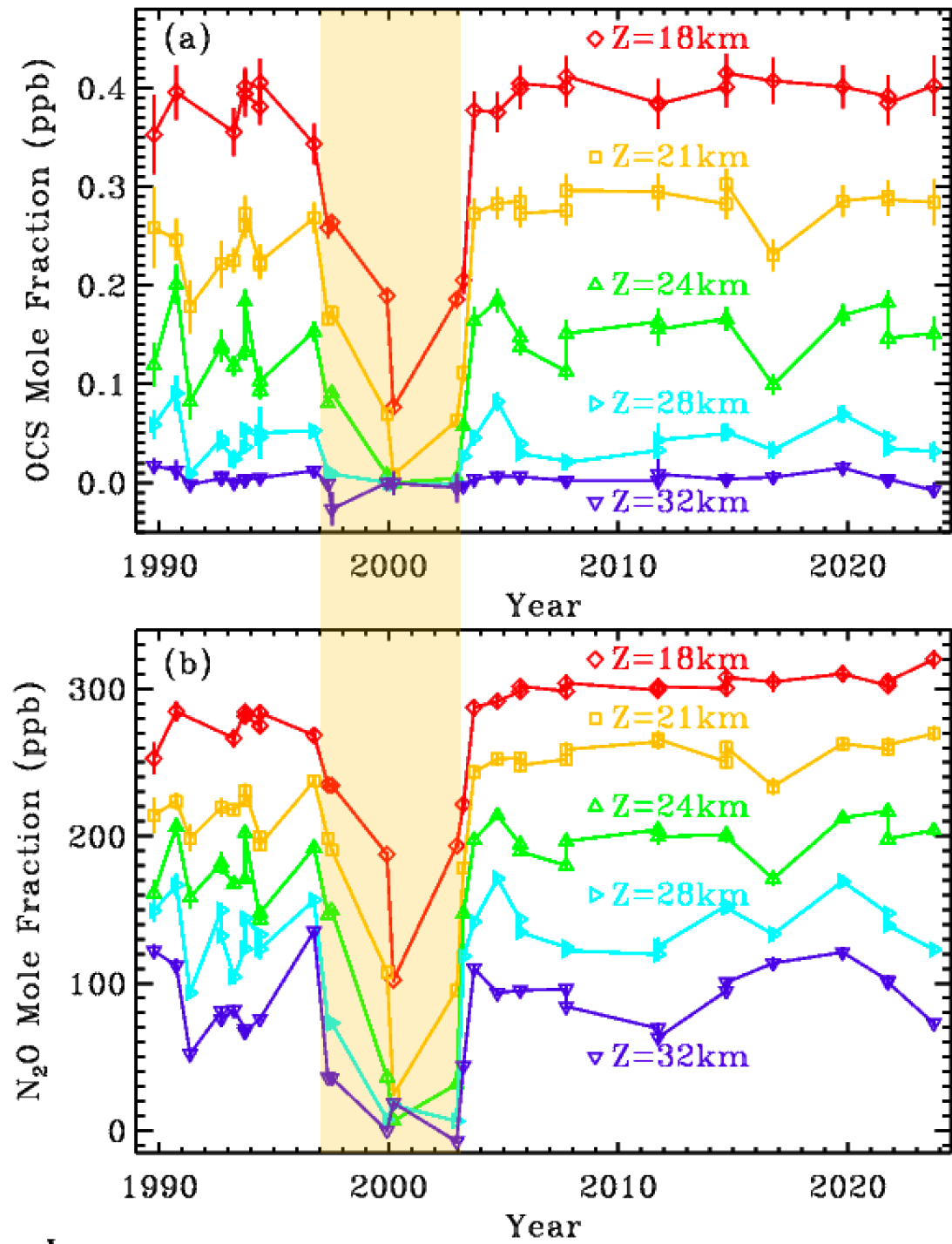
The fact that the OCS-N<sub>2</sub>O relationship is linear at lower altitudes (N<sub>2</sub>O > 150 ppb) means that here these gases both have lifetime greater than transport times. At higher altitudes the relationship becomes curved, since the OCS lifetime is shorter than N<sub>2</sub>O's, but remains compact. *Plumb and Ko (1992)*.



# OCS and N<sub>2</sub>O VMRs at fixed altitudes

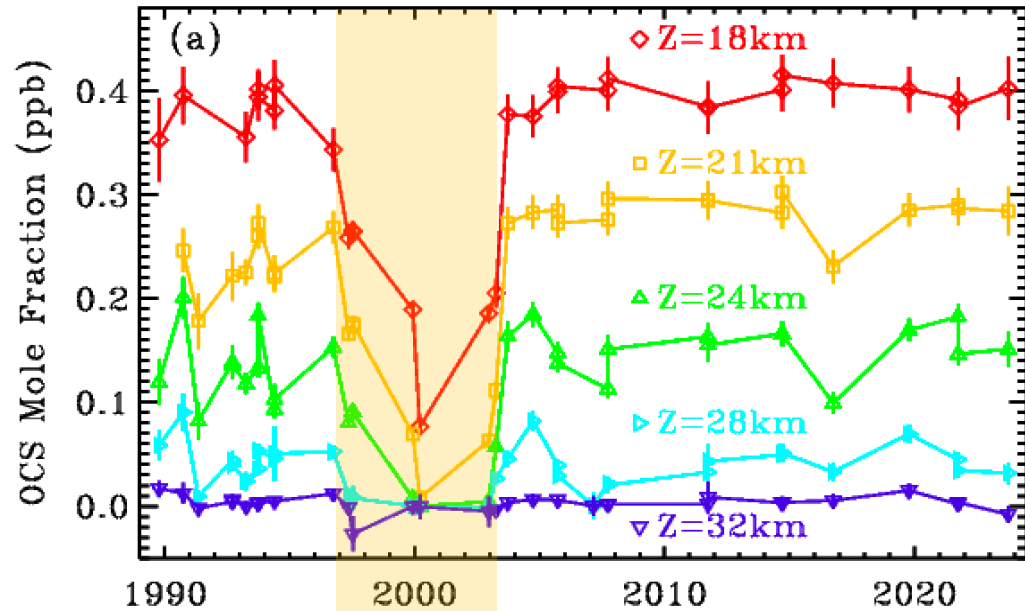
Behavior of N<sub>2</sub>O and OCS is qualitatively very similar. Reduced values for the high-latitude flights (yellow shading) and considerable flight-to-flight variations, even at 35N.

Due to the downward transport in the winter vortex, the N<sub>2</sub>O and OCS vmrs are down to zero in the late-1999, early 2000, and late 2022 flights at the higher altitudes.

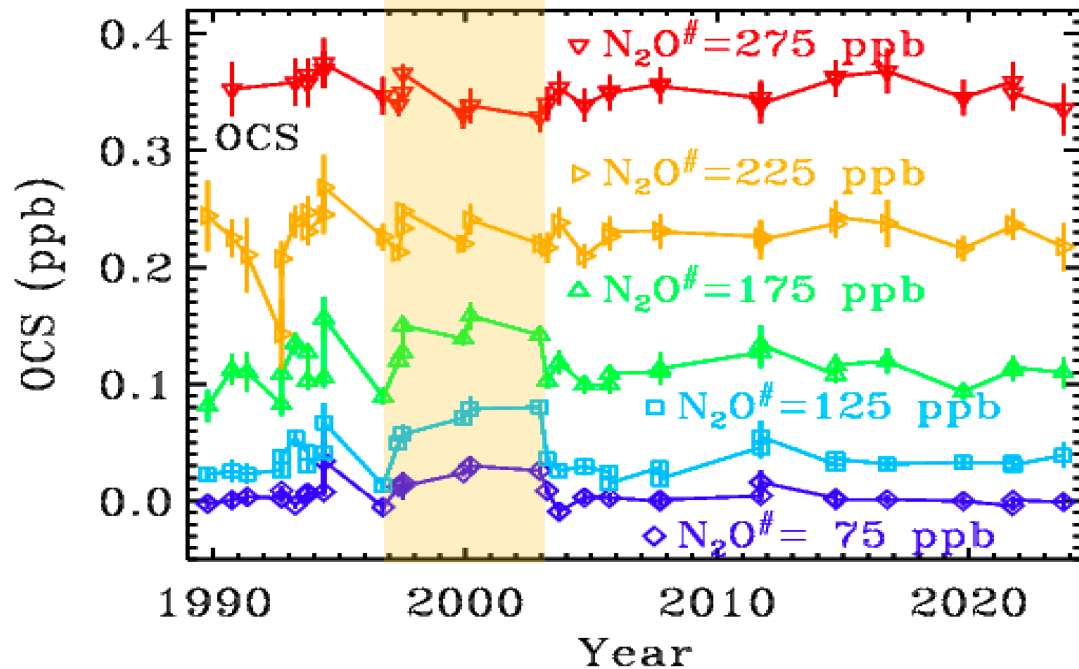


# OCS interpolated onto $N_2O^{2K}$ isopleths

Upper panel shows OCS interpolated onto fixed altitude levels, as shown earlier. There is considerable flight-to-flight variability, especially for the six high-latitude flights (yellow shading).



Lower panel shows OCS interpolated onto fixed  $N_2O$  isopleths: 75, 125, 175, 225 and 275 ppb. The flight-to-flight variation is reduced in comparison with the upper panel, allowing a more accurate trend determination. The high latitude flights fall into line with the 35N flights, at least at the lower altitudes.



Compared MkIV gas variations with those from ACE as reported by Schmidt et al. (2024)



Journal of Quantitative Spectroscopy and  
Radiative Transfer

Volume 325, October 2024, 109088

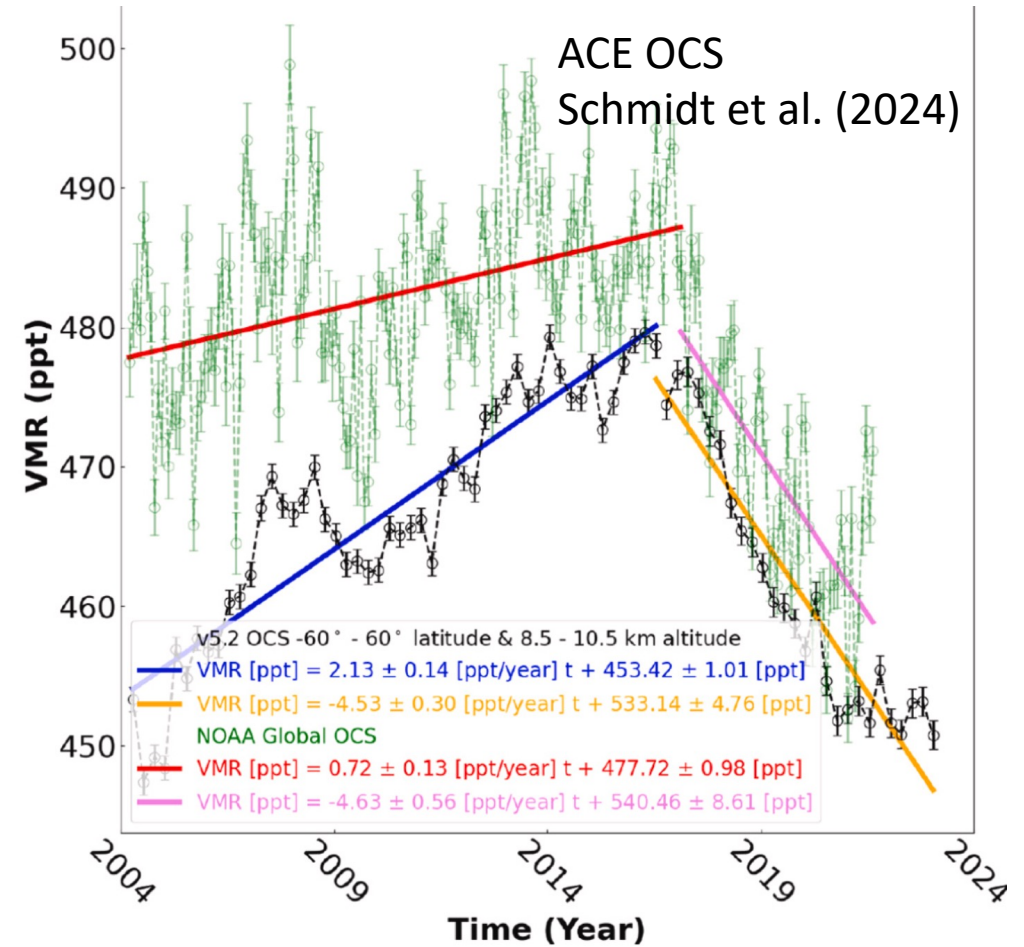
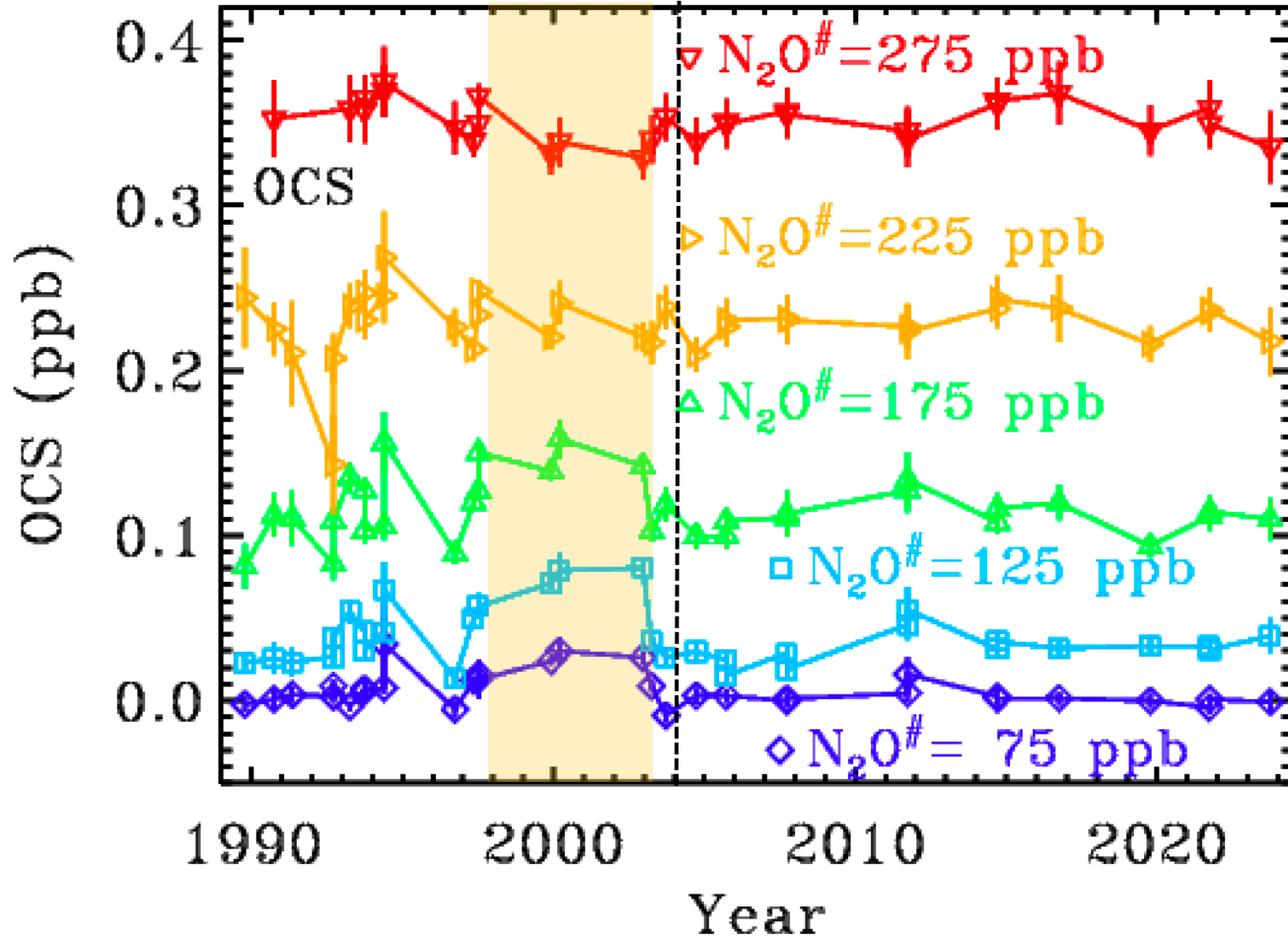


# Trends in atmospheric composition between 2004–2023 using version 5 ACE-FTS data

Matthew Schmidt <sup>a</sup>  , Peter Bernath <sup>b</sup> <sup>a</sup>, Chris Boone <sup>a</sup>, Michael Lecours <sup>a</sup>, Johnathan Steffen <sup>a</sup>

[Show more](#) 

# MkIV-ACE: OCS Trend comparison

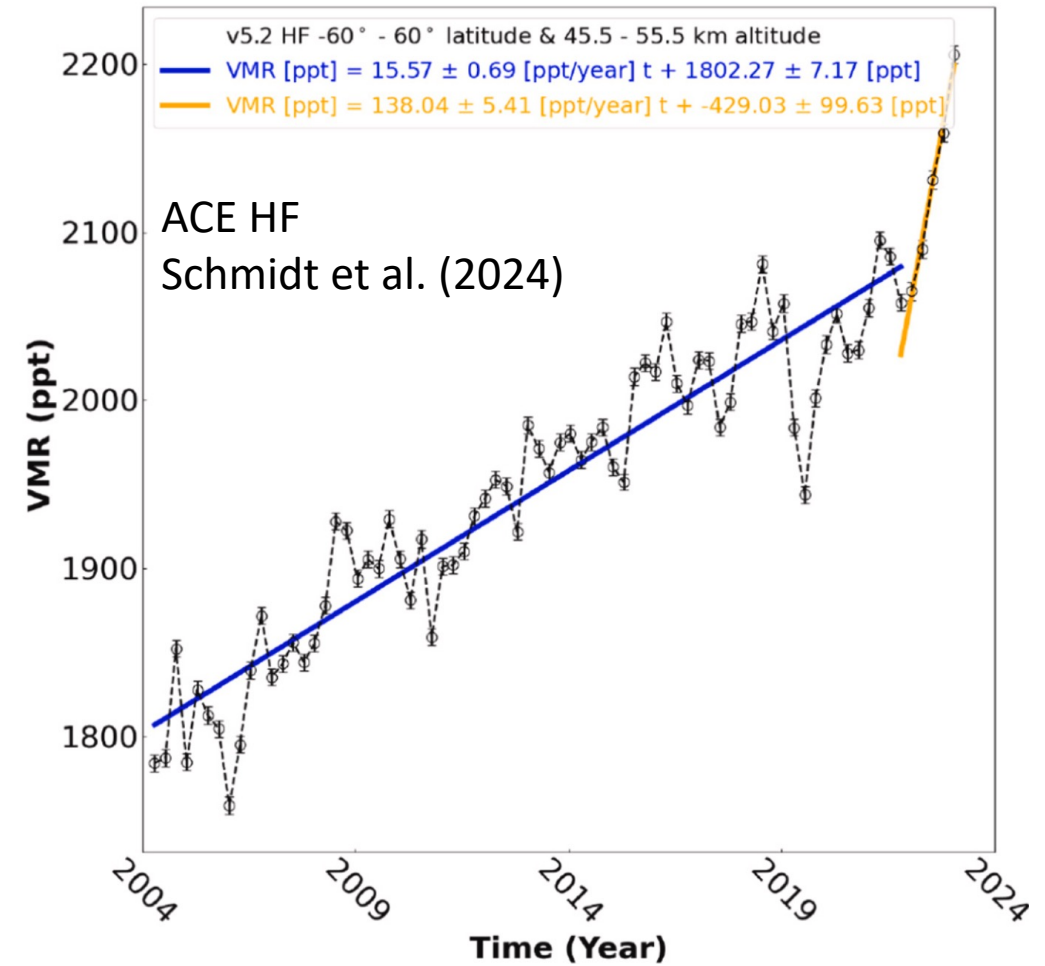
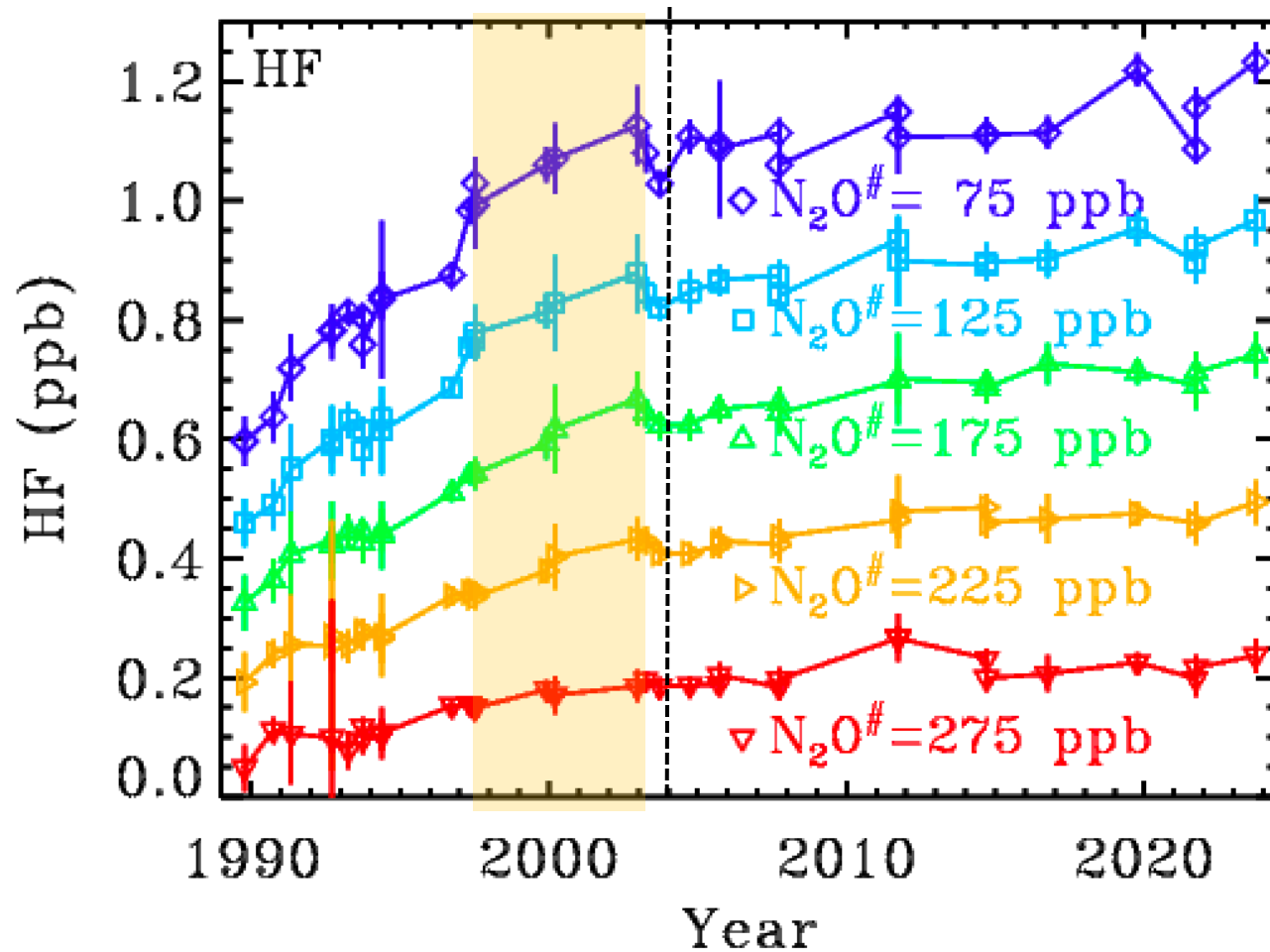


**Left:** MKIV OCS shows no significant trends in the stratosphere at any of the five  $N_2O$  isopleths/altitudes. Vertical dotted black line indicates start of ACE record.

**Right:** ACE shows a peak in OCS in 2017 over the 8.5 to 10.5 km altitude range, followed by a sharp decrease.

ACE OCS values are 30% larger than those of MKIV (partly due to lower altitude of ACE measurements)

# MkIV-ACE HF Trend Comparison

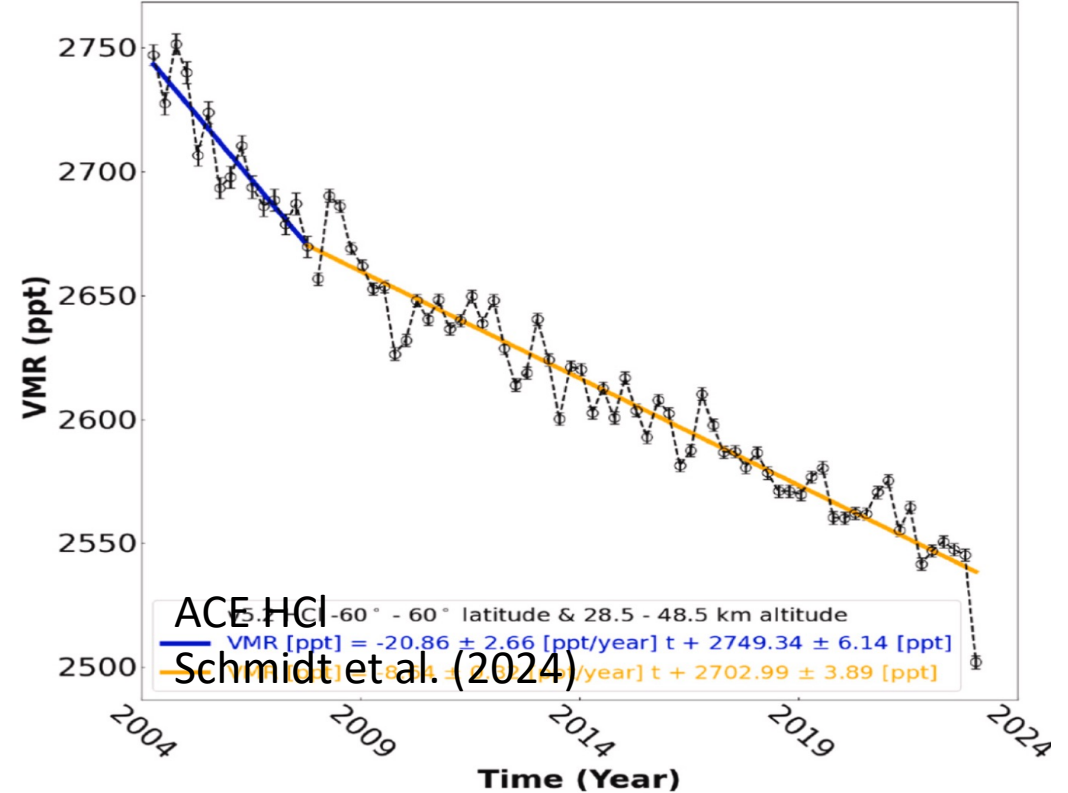
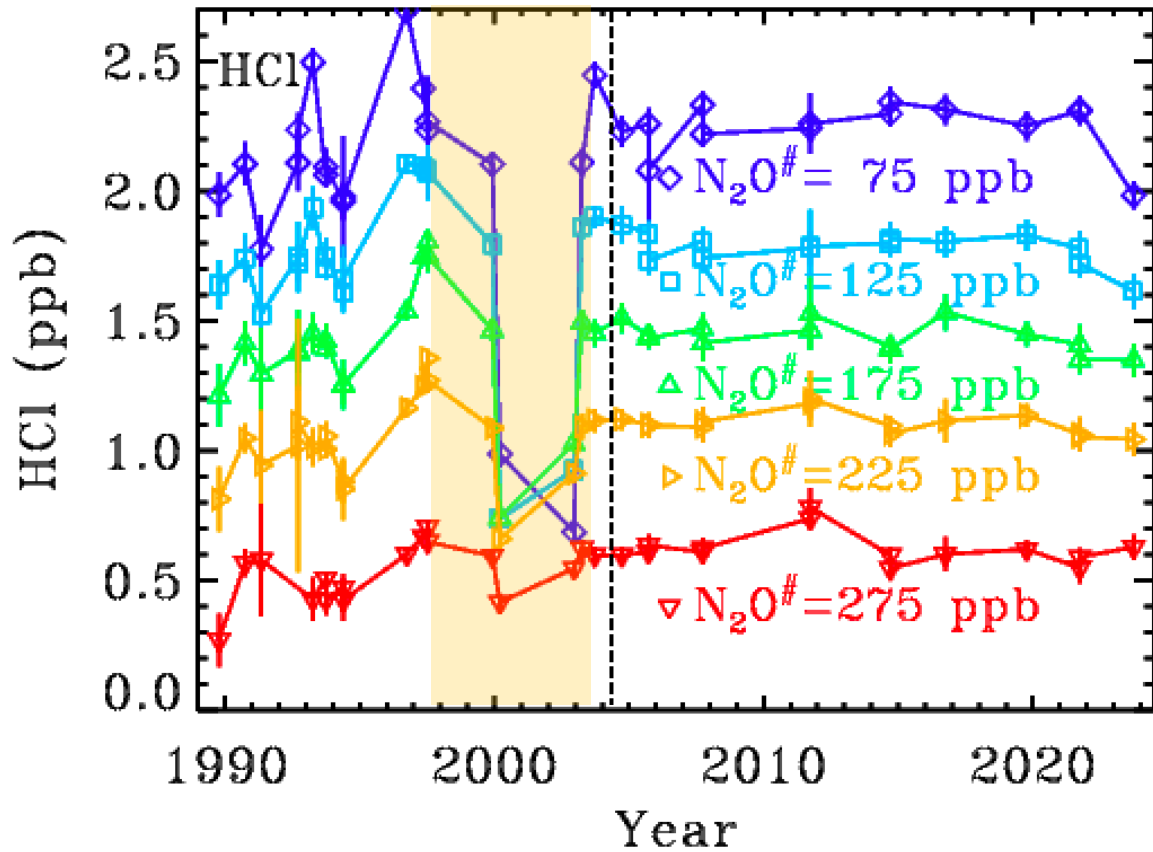


Left: Retrieved MKIV HF vmrs interpolated to various N<sub>2</sub>O isopleths. Large vmrs from 1997-2003 for high latitudes (Fairbanks and Esrange). The other flights were all from ~35N. HF has increased by more than a factor two 1989-2022, but has now slowed down.

Right: ACE HF vmrs 45-55 km altitude.



# MkIV-ACE HCl Trend Comparison

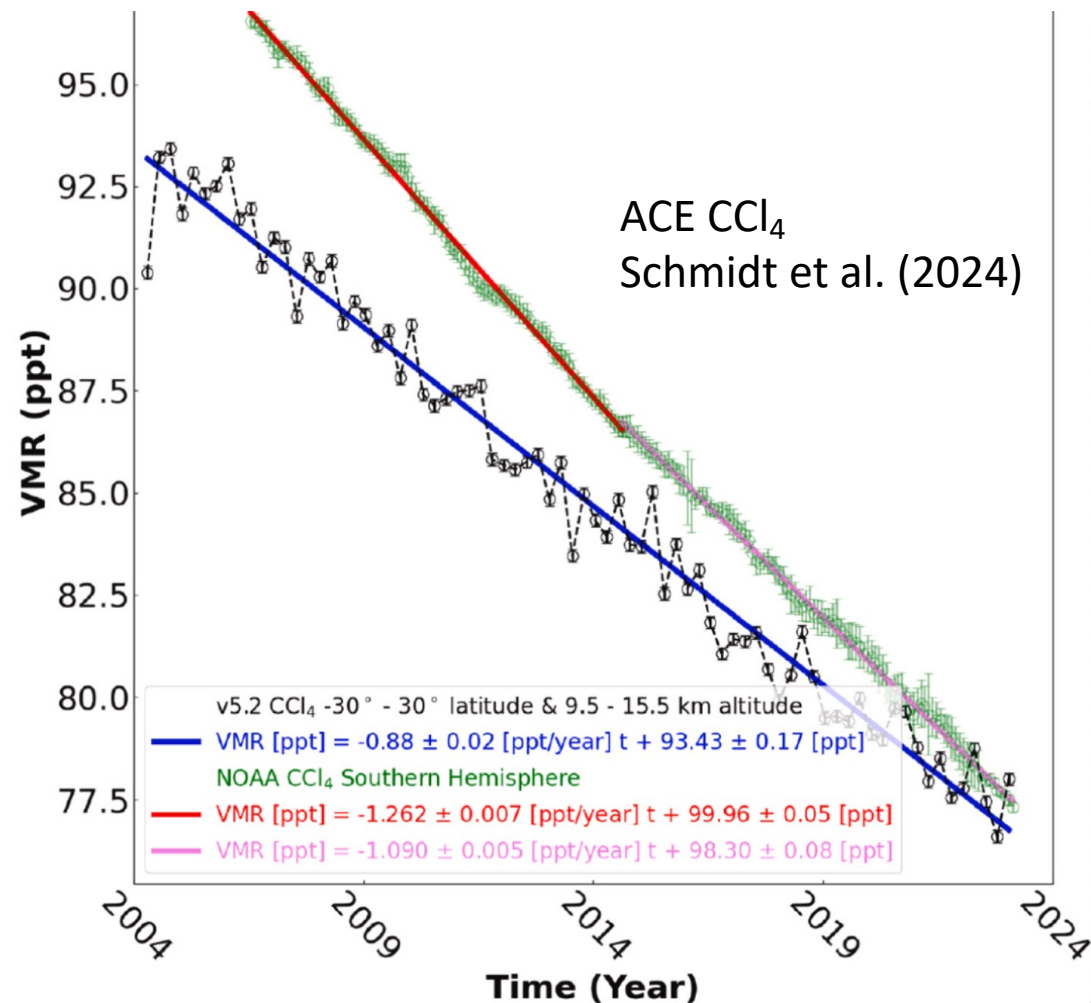
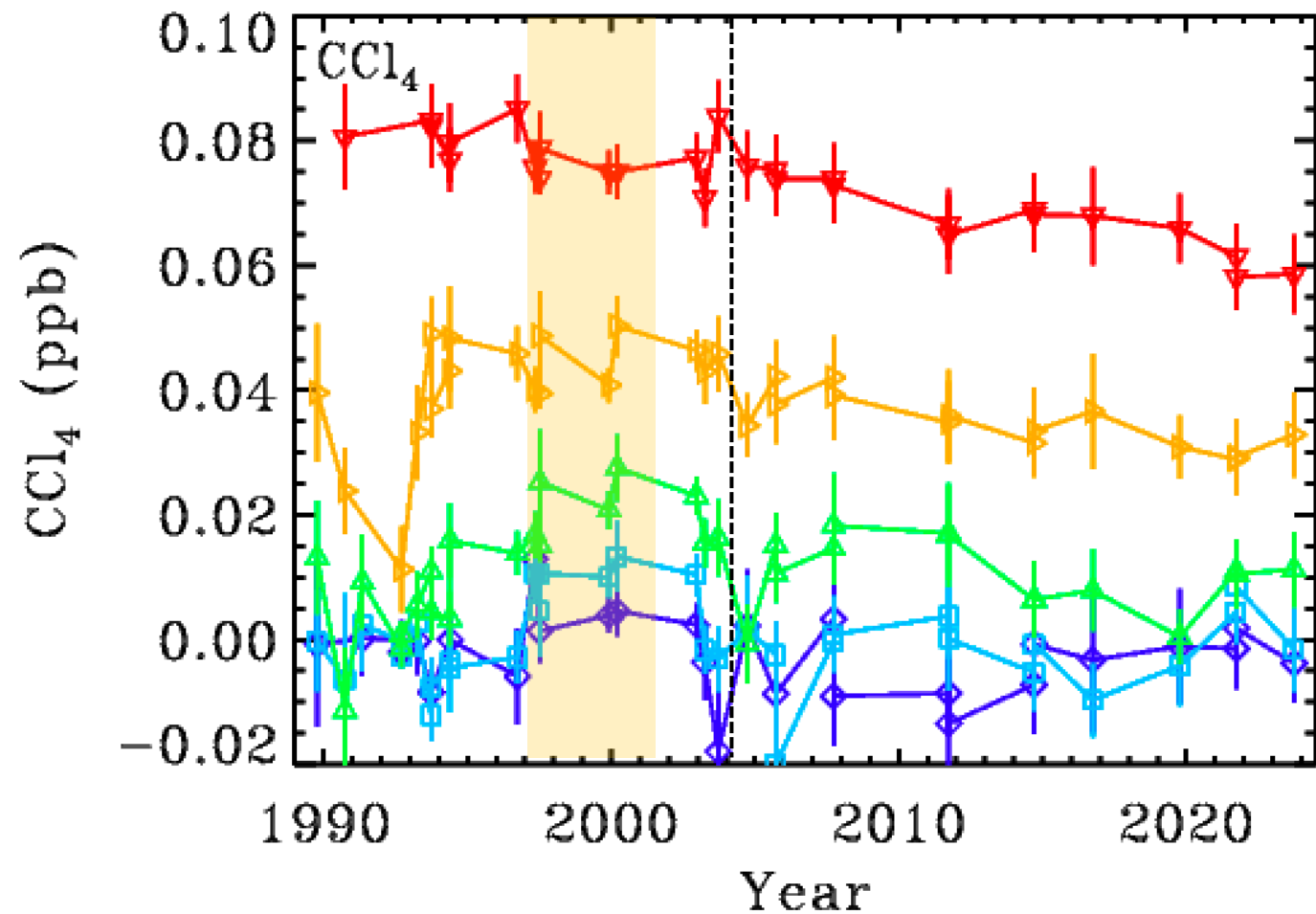


MkIV saw increasing HCl from 1989 to 2000. Two of four high-latitude flights in the winter vortex (yellow shading) show large heterogeneous loss of HCl.

The ACE HCl measurements (right panel) cover the 28.5—48.5 km altitude range, which is above the highest MKIV altitude range (75 ppb of  $N_2O$ ), and therefore provides slightly larger HCl VMRs.

ACE sees a 6% total decrease (from 2750 to 2585 ppt) over 16 years. Possibly inconsistent with MKIV, although different altitudes are sampled. Ground-based HCl columns saw increasing HCl from 2007-2012 in the NH (Mahieu et al, 2014).

# MkIV-ACE CCl<sub>4</sub> Trend Comparison

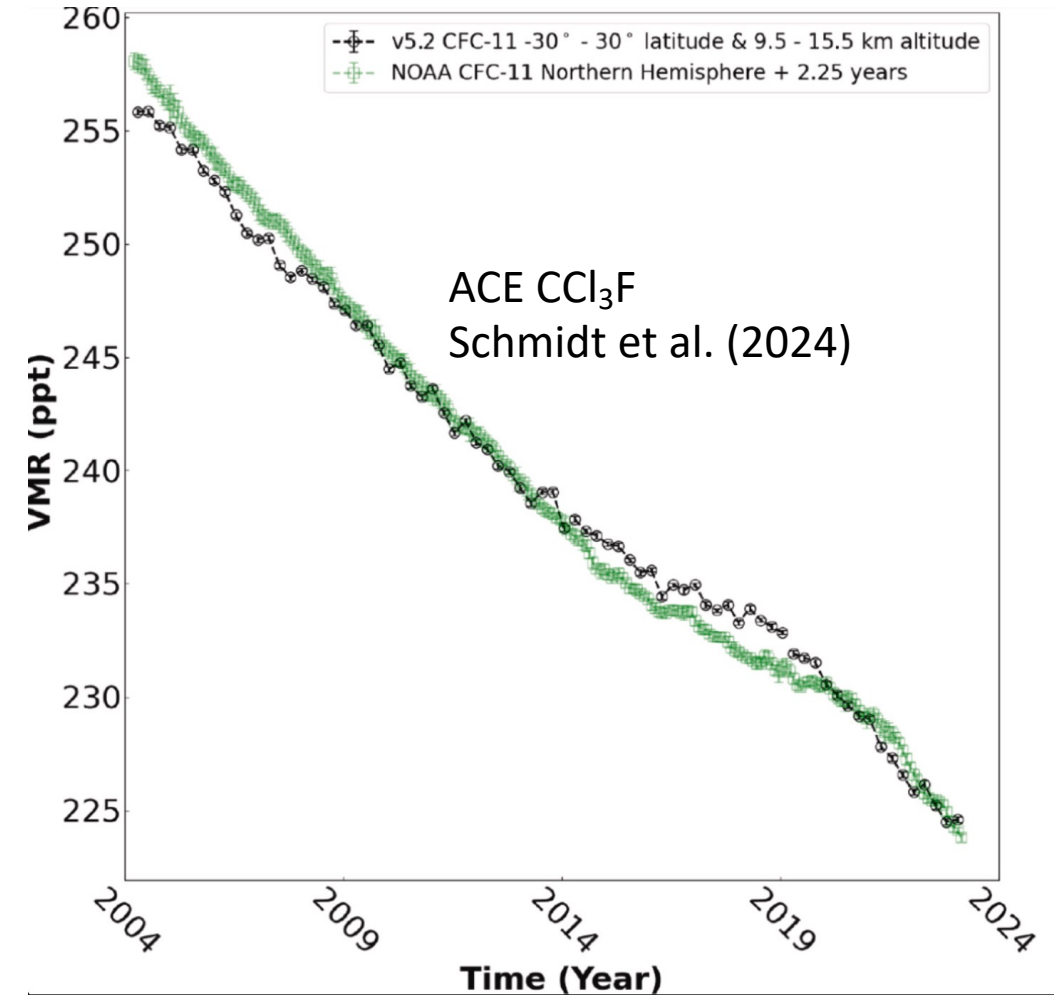
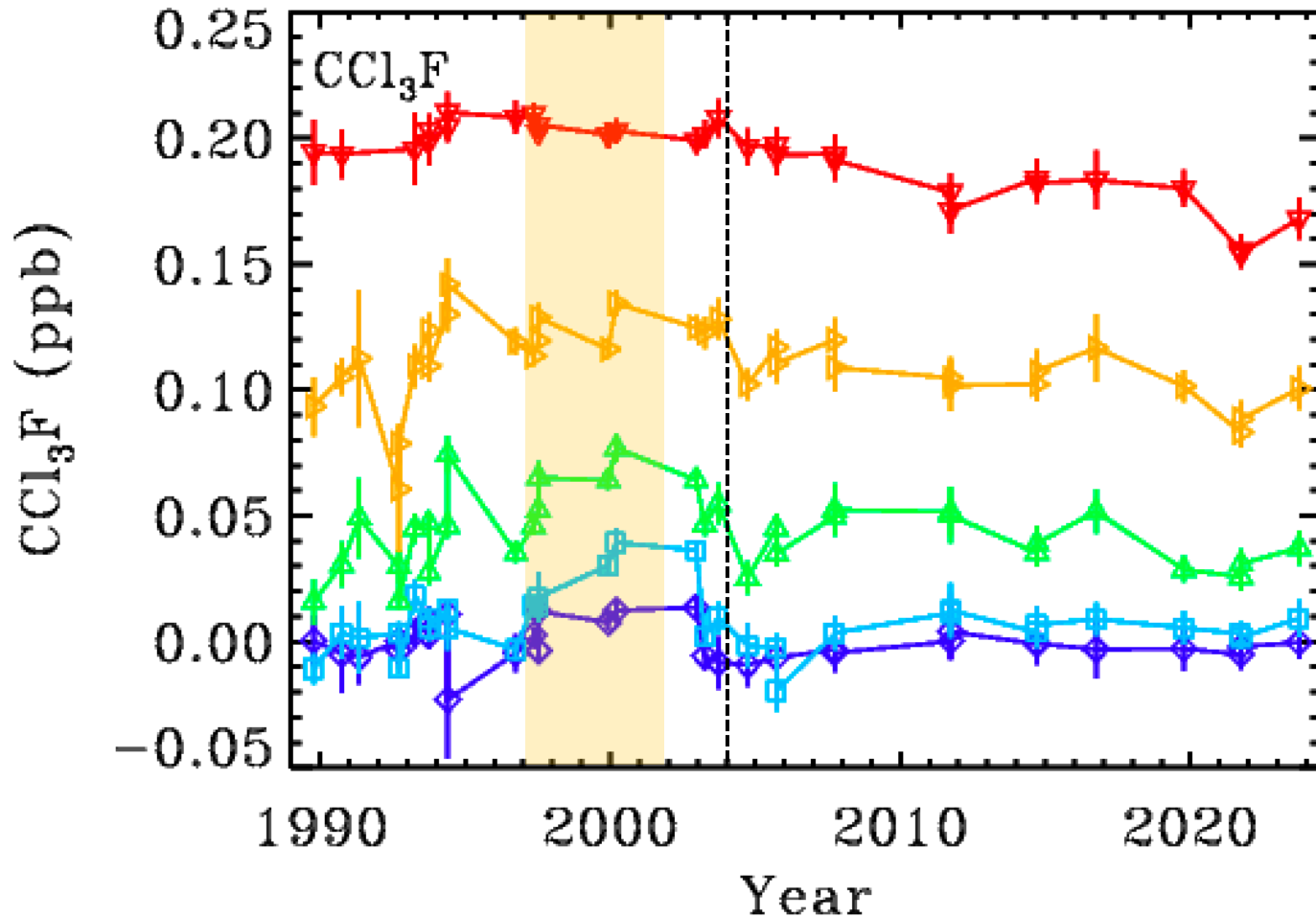


MkIV CCl<sub>4</sub> peaked around 1995 at lowest altitude (red). Has been decreasing since.

ACE CCl<sub>4</sub> covers the 10–15 km altitude. They show a steady decrease since 2004 .

ACE CCl<sub>4</sub> VMRS are 40% larger than those of the lowest (250 ppb N<sub>2</sub>O) MKIV .

# MkIV-ACE CCl<sub>3</sub>F Comparison

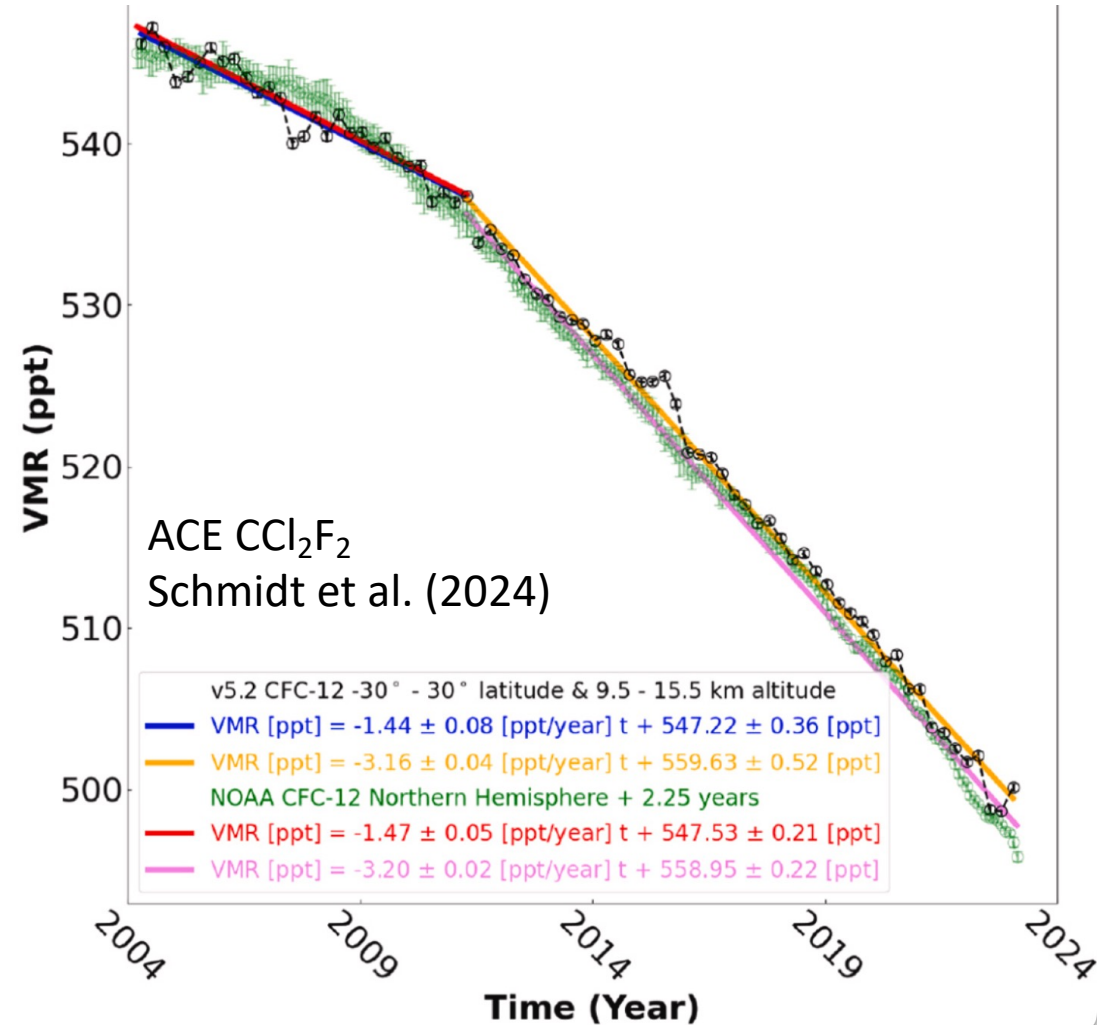
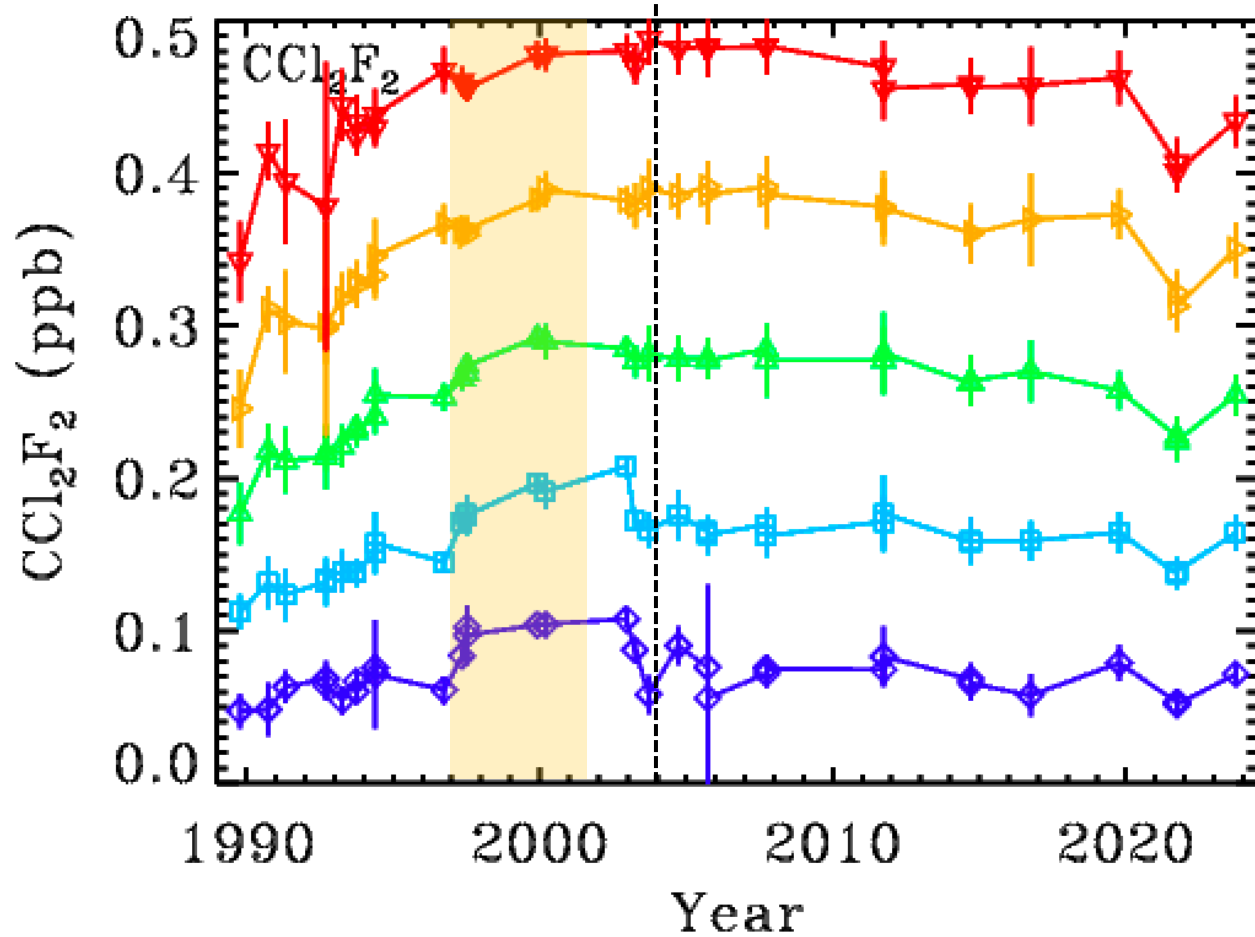


MkIV CCl<sub>3</sub>F peaked around 1994 at lowest altitude. Has been decreasing since.

ACE CCl<sub>3</sub>F covers the 10—15 km altitude. They show a steady decrease since 2004 .

ACE CCl<sub>3</sub>F VMRS are larger than those of MKIV because they represent lower altitudes.

# MkIV-ACE CCl<sub>2</sub>F<sub>2</sub> Trend Comparison

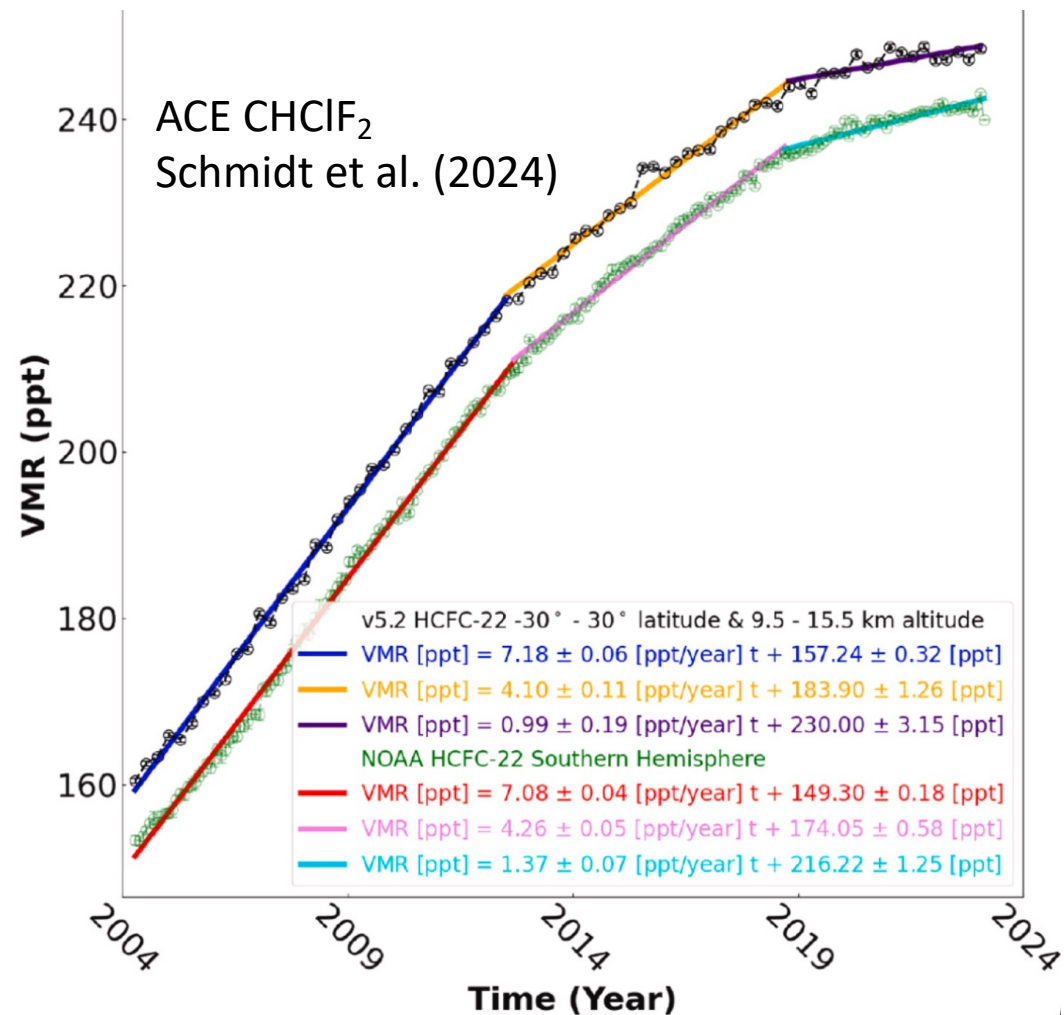
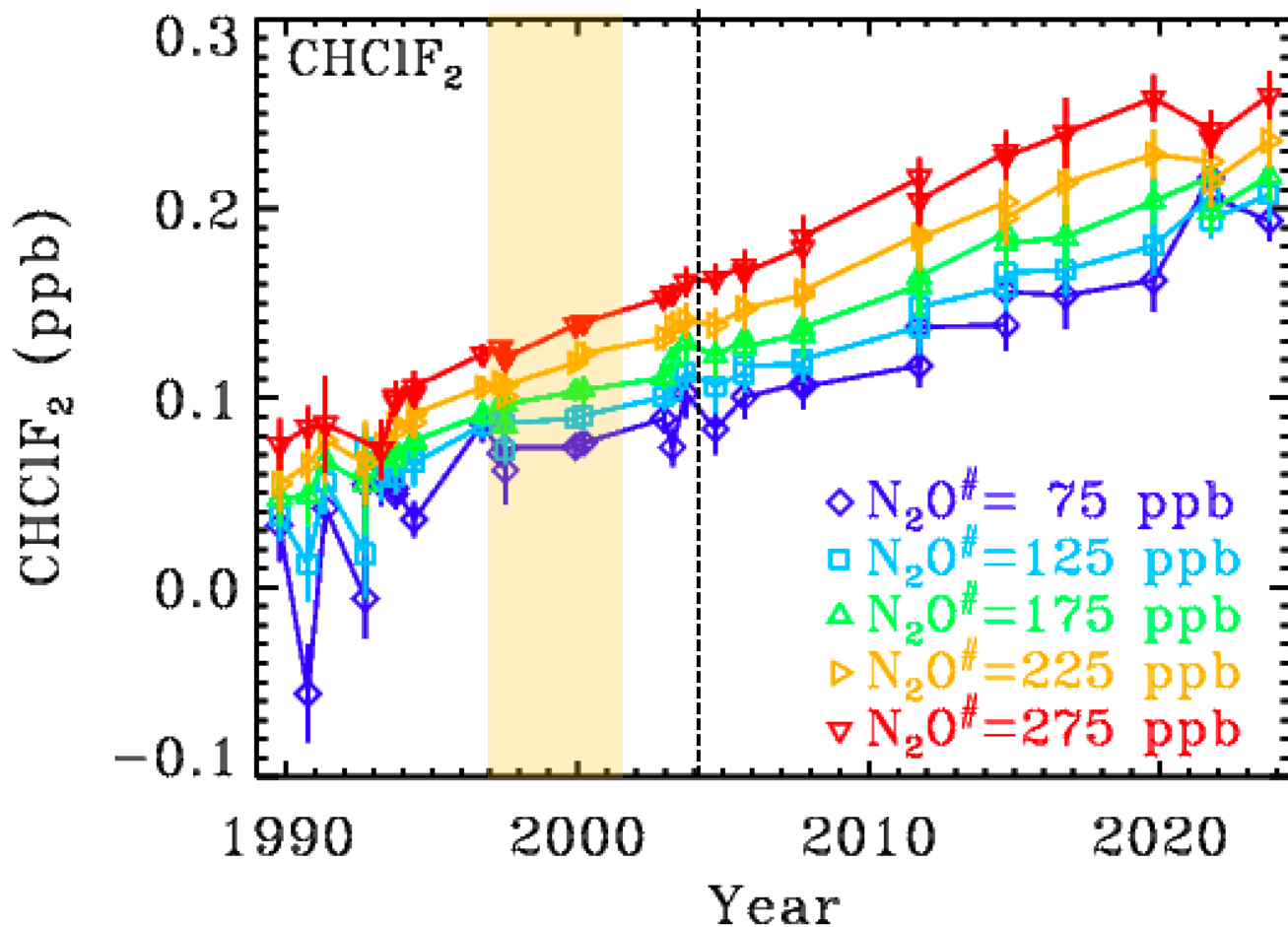


MkIV CCl<sub>2</sub>F<sub>2</sub> increased in the 1990s, peaked around 2004. Has been decreasing since.

ACE CCl<sub>2</sub>F<sub>2</sub> covers the 5—10 km altitude, which is lower than 275 ppb N<sub>2</sub>O. They show a linear decrease since 2011.

ACE CCl<sub>2</sub>F<sub>2</sub> VMRS are larger than those of MKIV because they represent lower altitudes.

# MkIV-ACE CHClF<sub>2</sub> Trends

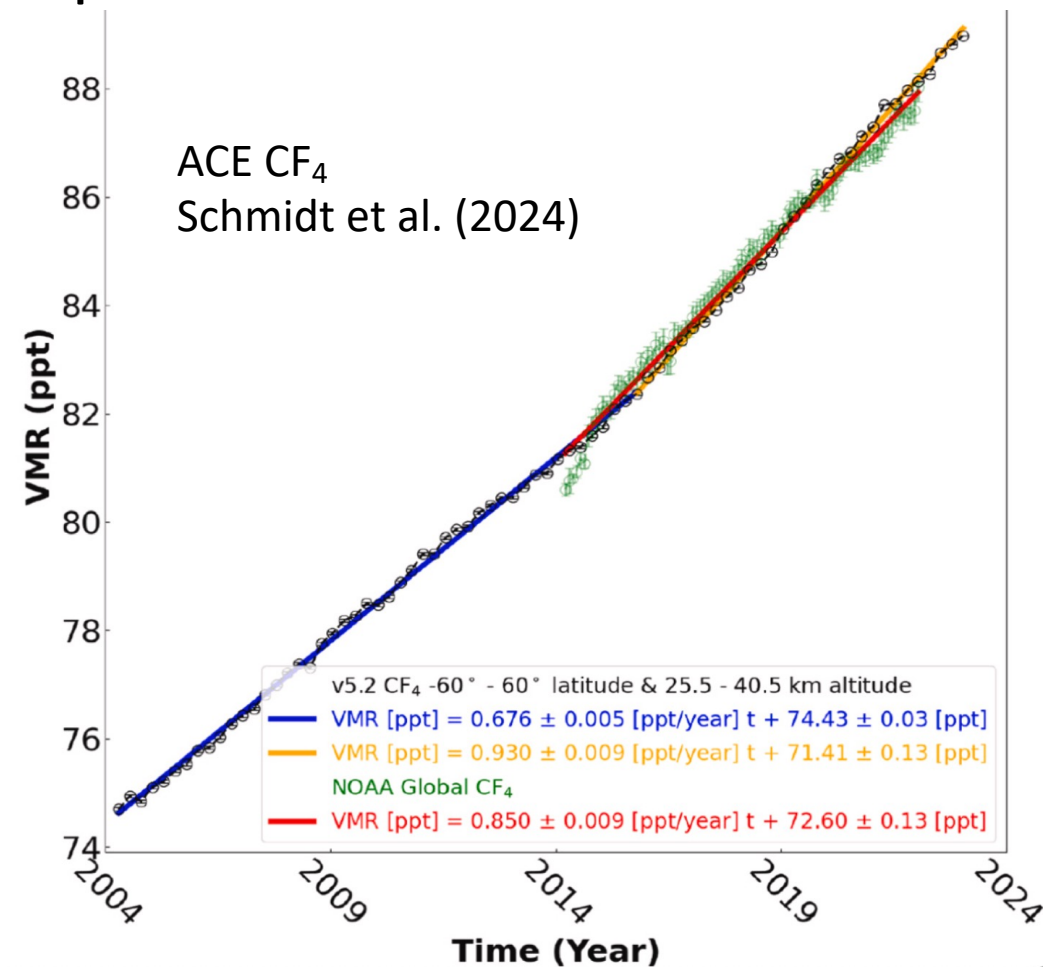
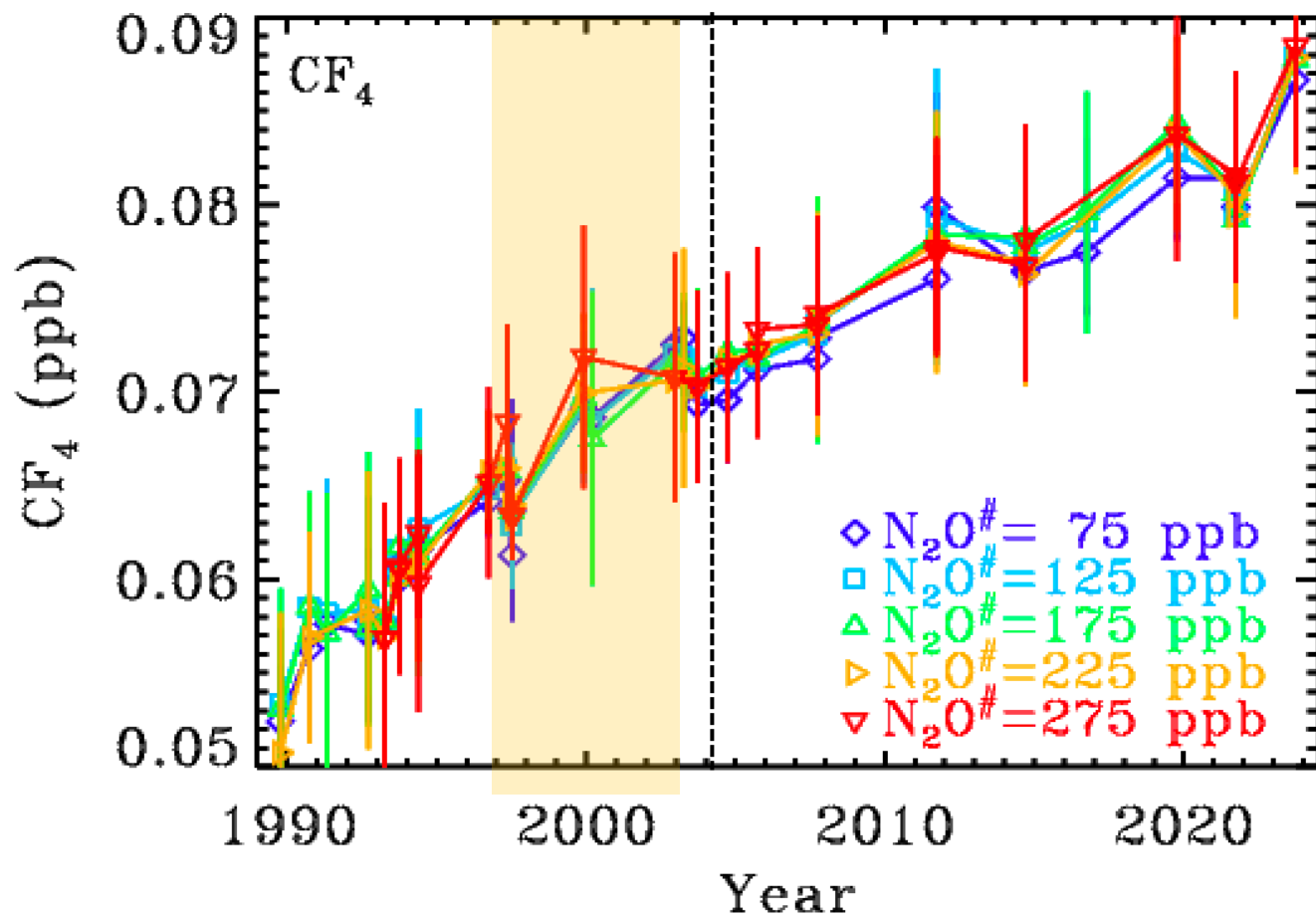


MkIV CHClF<sub>2</sub> has tripled since 1989 with an almost linear growth.

ACE CHClF<sub>2</sub> show a slowing rate of increase since 2004.

ACE CHClF<sub>2</sub> VMRS are similar to those of MKIV at the N<sub>2</sub>O=250 ppb level (red), despite representing lower altitudes (5-10 km).

# MkIV-ACE CF<sub>4</sub> Trend Comparison

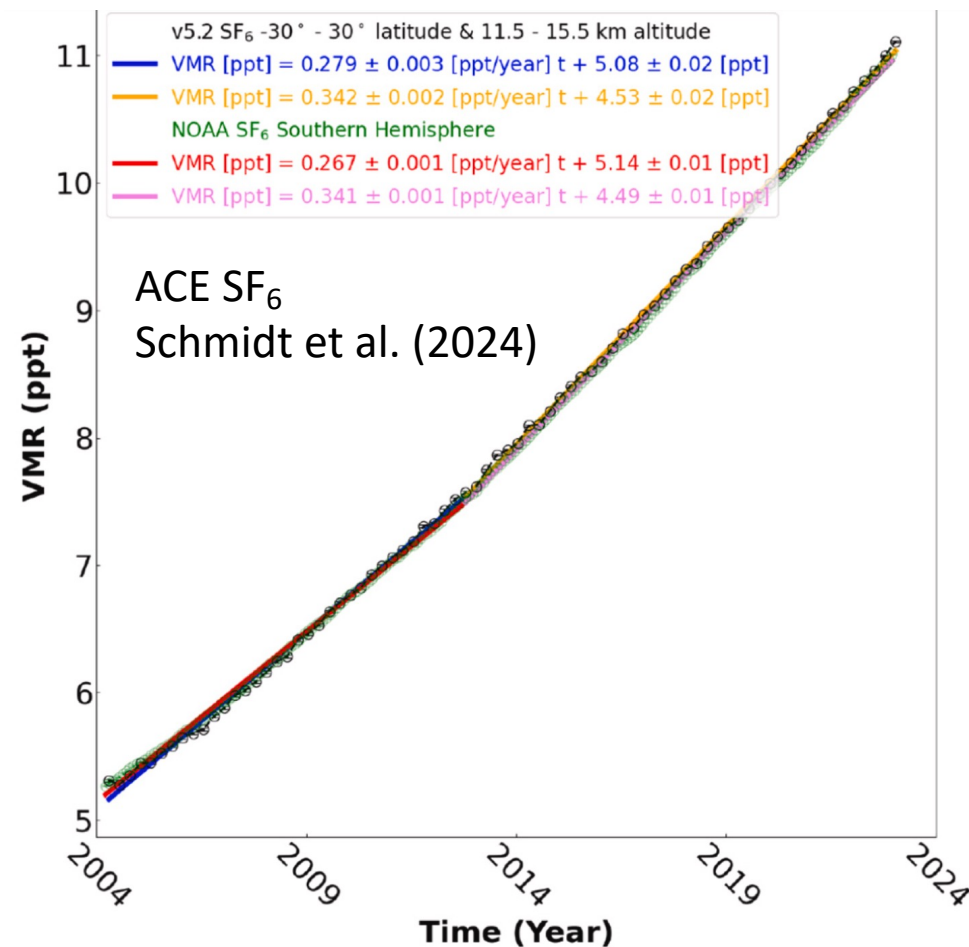
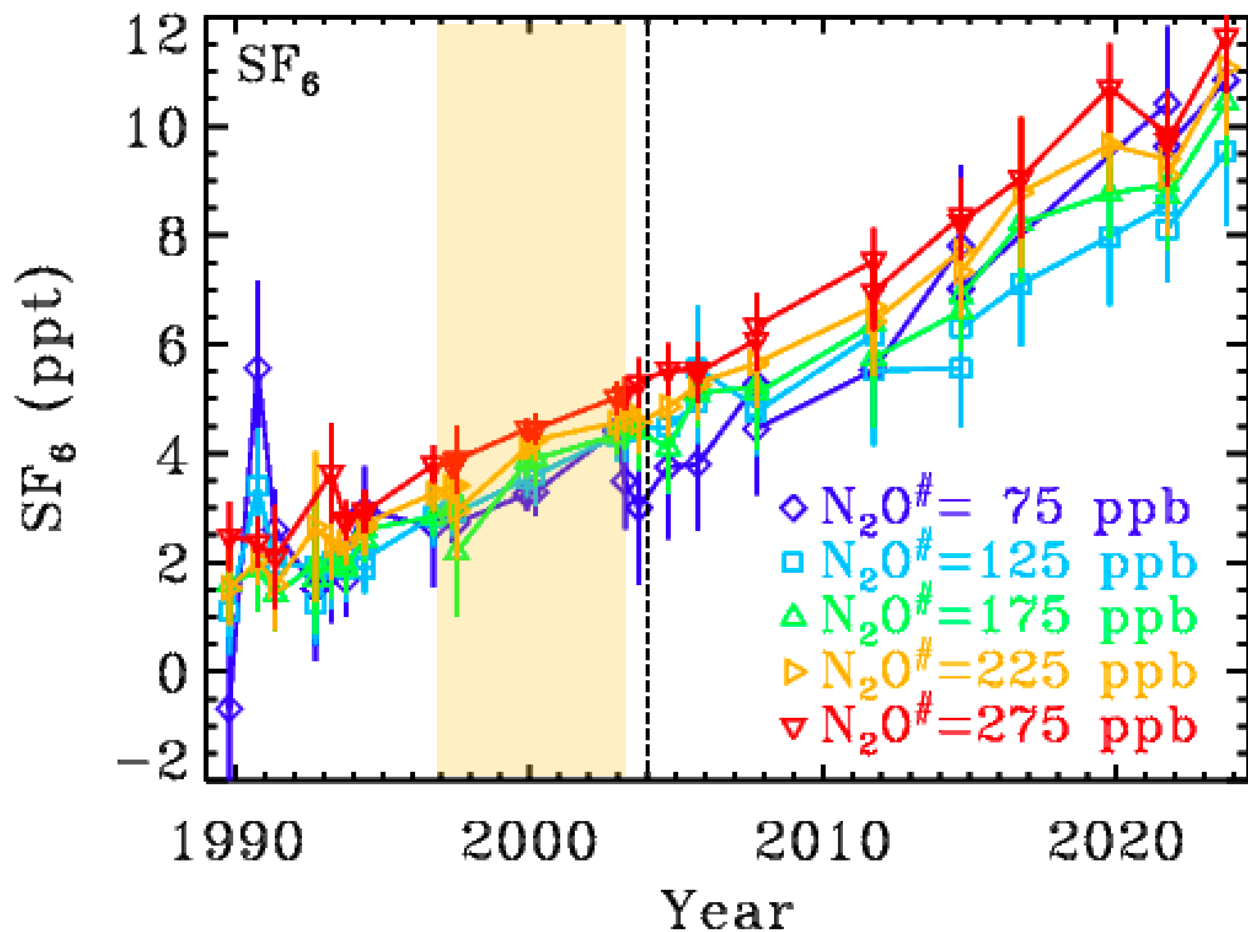


MkIV CF<sub>4</sub> has nearly doubled since 1989 with an almost linear growth. VMRs are noisy at the higher altitudes N<sub>2</sub>O=100 ppb (~30km), especially in the early years.

ACE CF<sub>4</sub> 25-40 km show an almost constant rate of increase 2004-2015, then a slightly faster increase since 2015.

ACE CF<sub>4</sub> VMRS are similar to those of MKIV at the N<sub>2</sub>O=275 ppb level in 2004

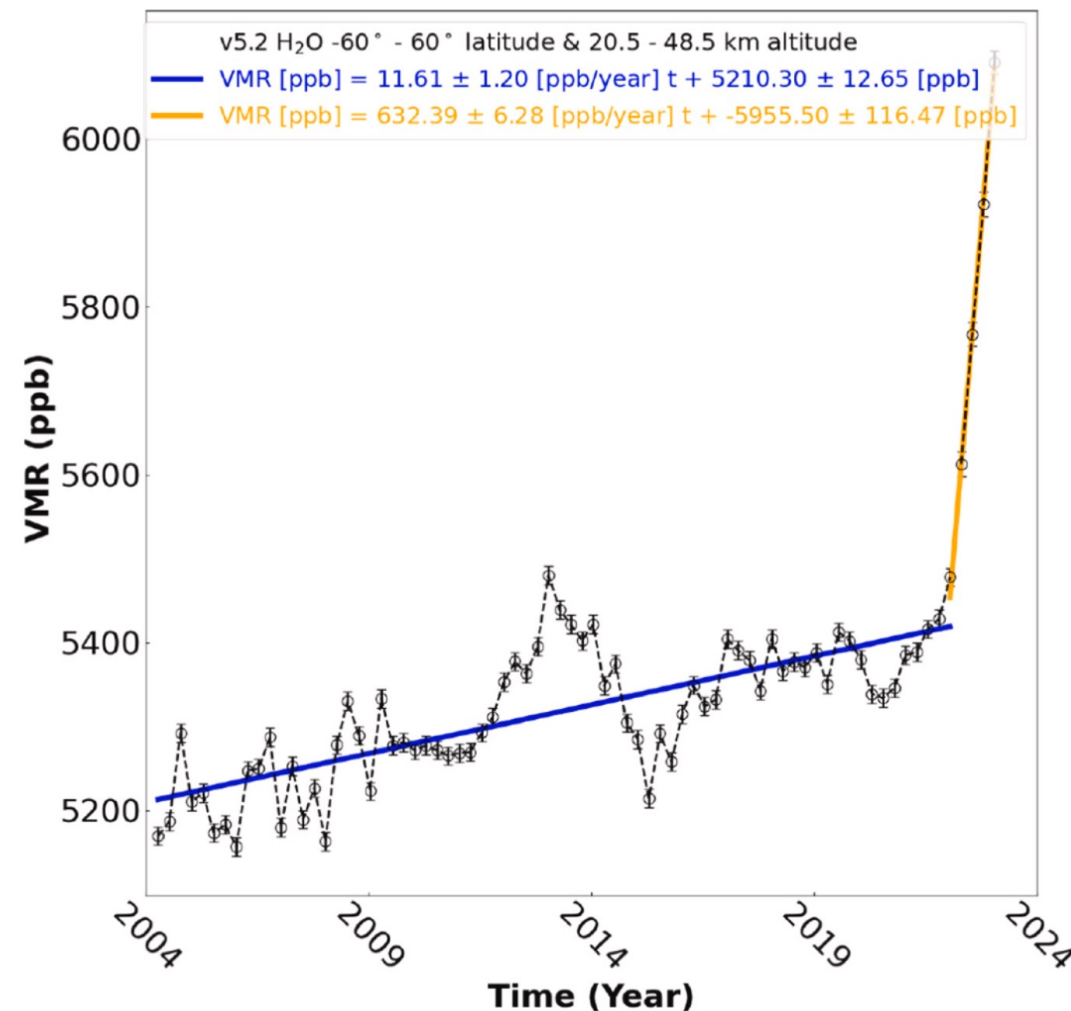
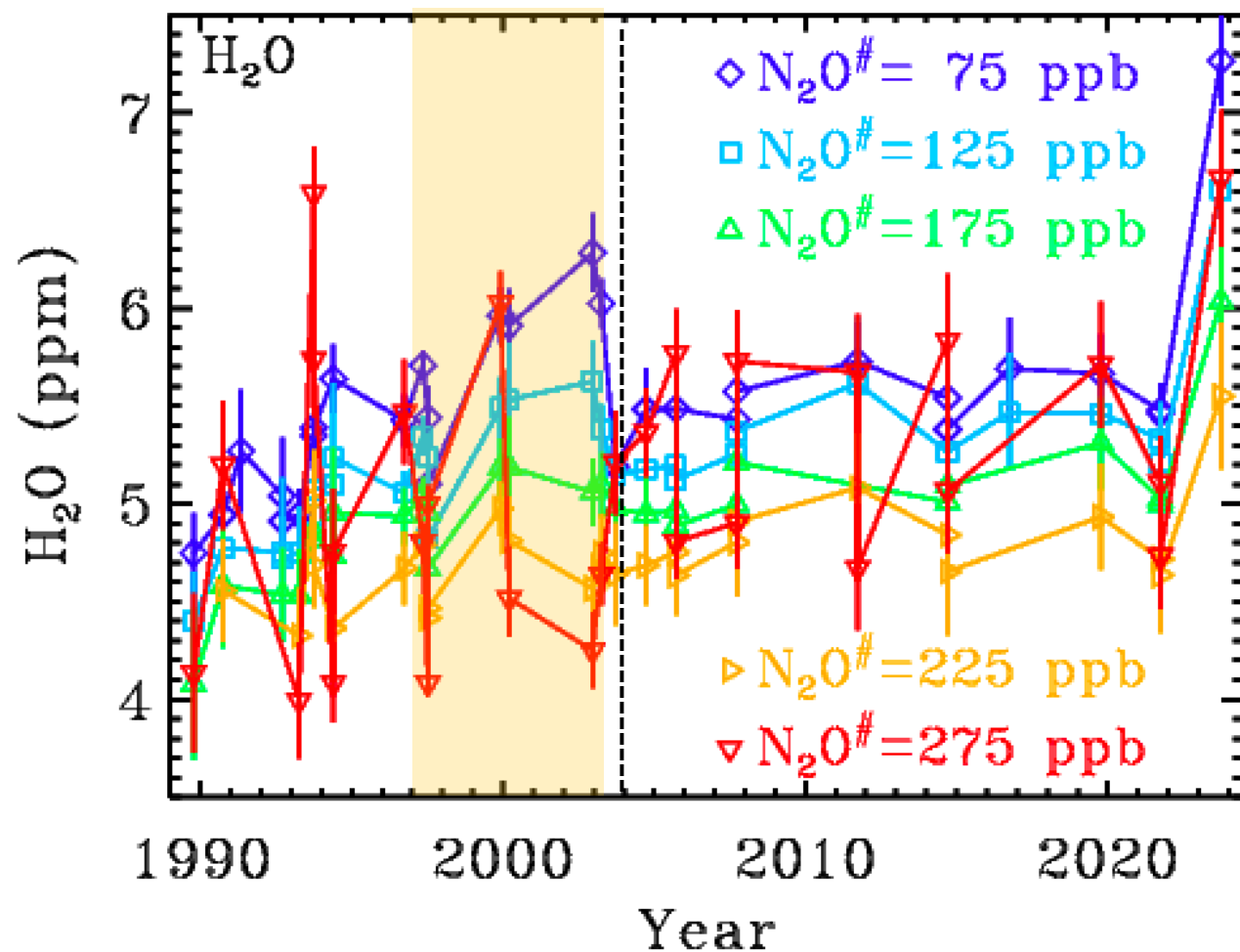
# MkIV-ACE SF<sub>6</sub> Trend Comparison



MkIV SF<sub>6</sub> has quintupled since 1989. from 2 ppt to 10 ppt, with a slightly increasing rate of growth. VMRs are noisy at the higher altitudes N<sub>2</sub>O=75 ppb (~30km), especially in the early years.

ACE SF<sub>6</sub> averaged over 11.5 to 15.5 km show similar values to the red (275 ppb N<sub>2</sub>O) MkIV curve.

# MkIV-ACE H<sub>2</sub>O Trend Comparison

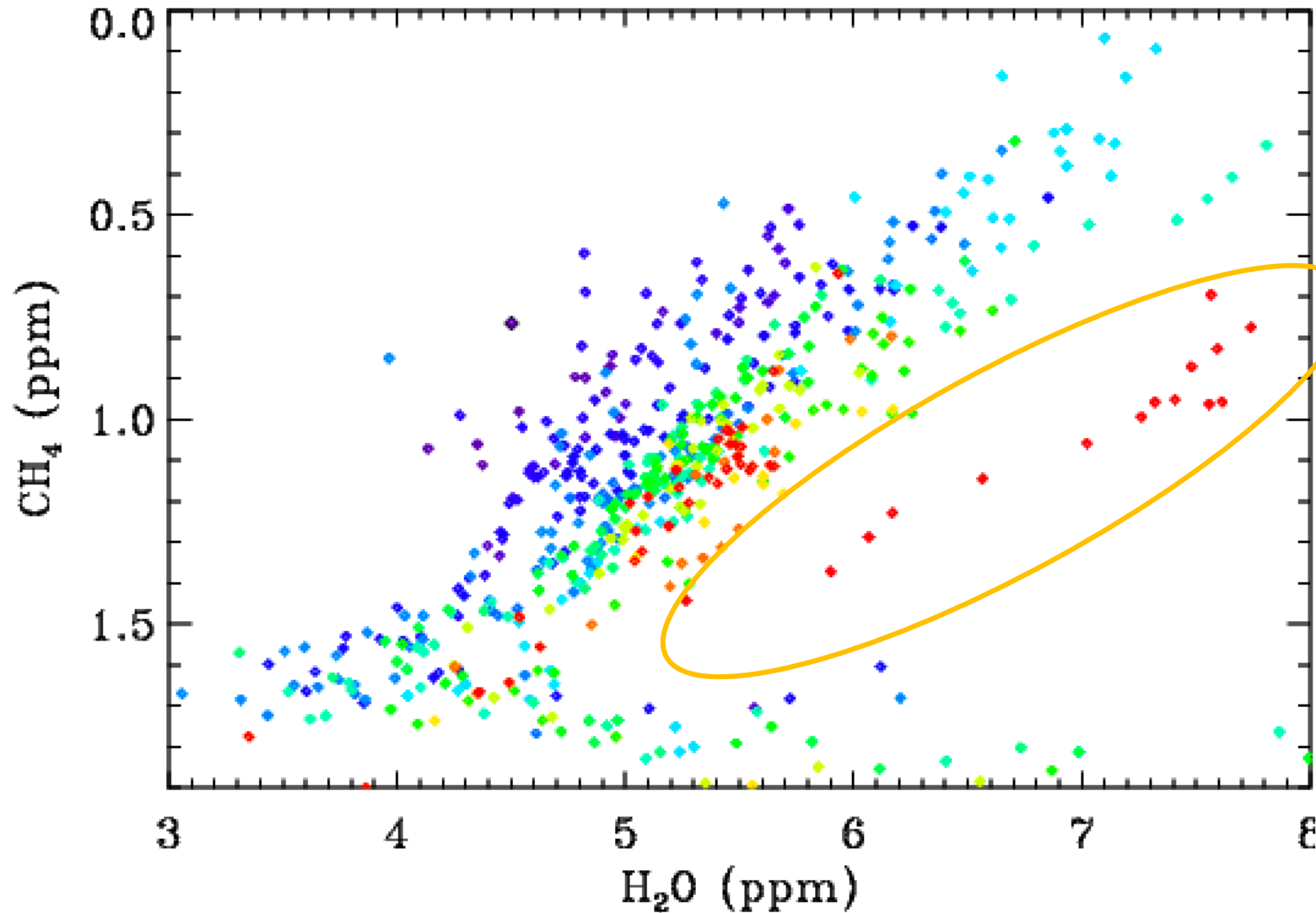


Left: MkIV stratospheric H<sub>2</sub>O increased from 1989 to 2000. Then, fairly constant until the Hunga Tunga eruption in Jan 2023.

Right: ACE H<sub>2</sub>O show a significant increase in the 20-48 km altitude range between 2004 and 2022. Then a spike in 2023 due to Hunga Tunga.



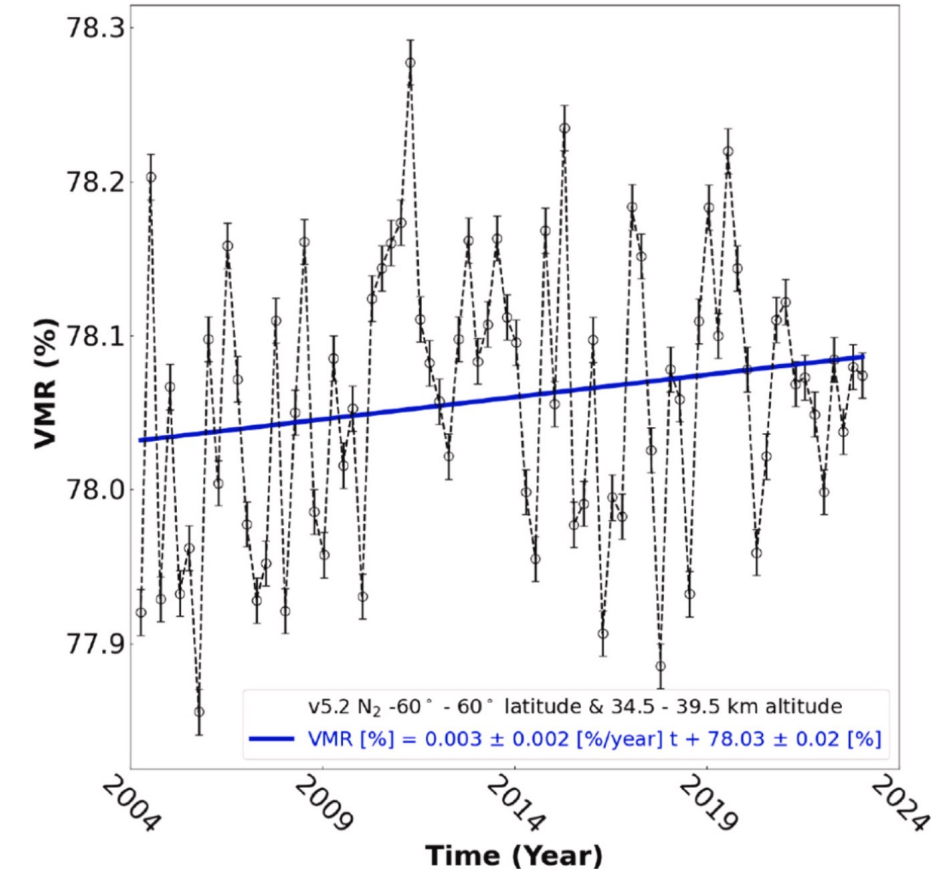
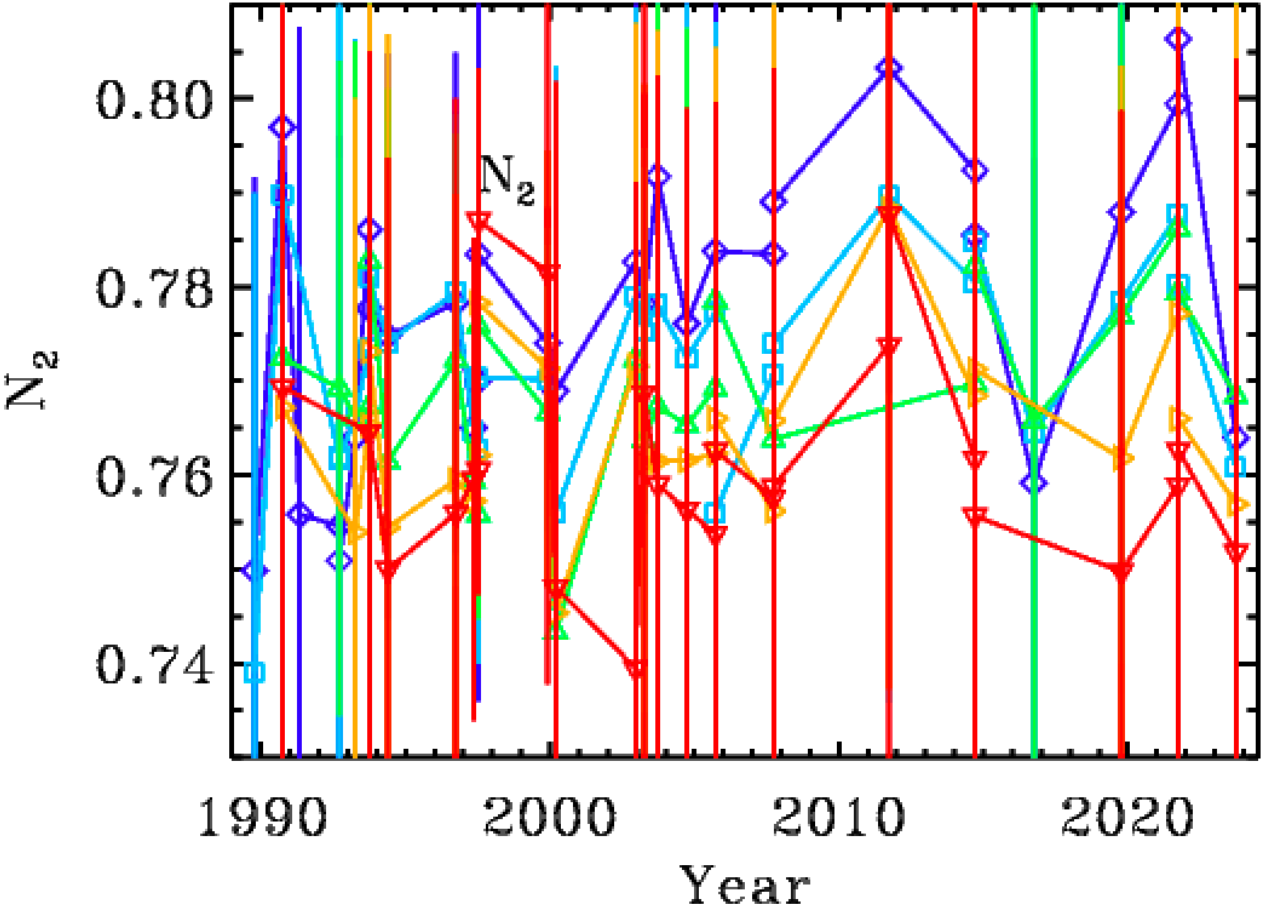
# H<sub>2</sub>O / CH<sub>4</sub> correlation plot color coded by year (2023 is red)



The 2023 points inside the oval show a H<sub>2</sub>O enhancement of 1 ppm in the lower strat, increasing to 1.5 ppm in the upper strat.

This proves that the 2023 H<sub>2</sub>O enhancement was not due to transport.

# MkIV-ACE N<sub>2</sub> Trend Comparison



Left: MkIV N<sub>2</sub> mole fraction is constant at about 0.77. No trend over time

Right: ACE N<sub>2</sub> averaged over 35-40 km altitude, is constant at 0.780 over the 28-32 km altitude range.

# Summary and Conclusions

ACE measurements of the long-term trends Schmidt et al. (2024) are highly precise due to the large number of occultations and in some cases the broad vertical averaging. Currently, no ACE trend information on different altitude ranges.

MkIV has only ~1 occultation per year with large flight-to-flight differences that exceed error bars. Need to “sacrifice” N<sub>2</sub>O profiles to remove effects of differences of airmass origin. Can’t average them away like ACE. Using N<sub>2</sub>O adds some noise (from N<sub>2</sub>O) to the gas trends, but for long-lived gases this is usually smaller than the dynamical effects that are removed.

Comparison of absolute VMR values between MkIV and ACE is difficult due to the different altitudes presented (Need to interpolate ACE data onto same N<sub>2</sub>O isopleths).

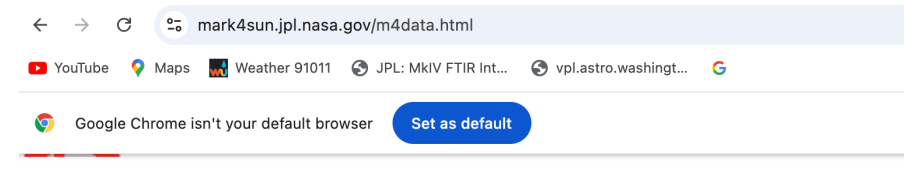
Compared trends between MkIV and ACE seem reasonable so far.

All MKIV flights were analyzed with the same software version and linelist.

The MKIV balloon profiles used in this presentation are available from:  
[https://mark4sun.jpl.nasa.gov/data/mkiv/m420230927\\_all\\_balloon.ames](https://mark4sun.jpl.nasa.gov/data/mkiv/m420230927_all_balloon.ames)

MkIV analysis assumes a compact Gas-N<sub>2</sub>O relationship not varying with latitude.

***Funded by NASA’s Upper Atmosphere Composition Observations Program***



## MkIV Balloon

	Ames-1001-format	Spreadsheet-format
All flights as of 2023 in one file:	<a href="#">m420230927_all_balloon.ames</a>	<a href="#">m420230927_all_balloon.ss</a>
All flights as of 2021 in one file:	<a href="#">m420210926_all_balloon.ames</a>	<a href="#">m420210926_all_balloon.ss</a>
All flights as of 2019 in one file:	<a href="#">m420191007_all_balloon.ames</a>	<a href="#">m420191007_all_balloon.ss</a>
All flights as of 2016 in one file:	<a href="#">m420160927_all_balloon.ss.ames</a>	<a href="#">m420160927_all_balloon.ss</a>
BOS - Ft. Sumner, New Mexico:	<a href="#">mkiv.28-sep-96.fts.ss.ames</a>	<a href="#">mkiv.28-sep-96.fts.ss</a>
ADEOS - Fairbanks, Alaska:	<a href="#">m419970508_fai_sunrise_r2.bal</a>	<a href="#">m419970508_fai_sunrise_r2.bal.ss</a>
POLARIS - Fairbanks, Alaska:	<a href="#">m419970708_fai_ascent_r1.bal</a> <a href="#">m419970708_fai_descent_r1.bal</a>	<a href="#">m419970708_fai_ascent_r2.bal.ss</a> <a href="#">m419970708_fai_descent_r2.bal.ss</a>
SOLVE - Esrangle, Sweden:	<a href="#">m419991203_esn_sunset_r1.bal</a> <a href="#">m420000315_esn_sunrise_r1.bal</a>	<a href="#">m419991203_esn_sunset_r1.bal.ss</a> <a href="#">m420000315_esn_sunrise_r1.bal.ss</a>
SOLVE II - Esrangle, Sweden:	<a href="#">m420021216_esn_sunrise_r1.bal</a> <a href="#">m420030401_esn_sunrise_r1.bal</a>	<a href="#">m420021216_esn_sunrise_r1.bal.ss</a> <a href="#">m420030401_esn_sunrise_r1.bal.ss</a>
BOS - Ft. Sumner, New Mexico:	<a href="#">m420030919_fts_sunset_r1.bal</a> <a href="#">m420040923_fts_sunset_r1.bal</a> <a href="#">m420050920_fts_sunset_r1.bal</a> <a href="#">m420070922_fts_sunset_r2.bal</a> <a href="#">m420070923_fts_sunrise_r2.bal</a> <a href="#">m420110923_fts_sunset_r1.ames</a> <a href="#">m420110924_fts_sunrise_r1.ames</a> <a href="#">m420140913_fts_sunset_r1.ames</a> <a href="#">m420140914_fts_sunrise_r1.ames</a>	<a href="#">m420030919_fts_sunset_r1.bal.ss</a> <a href="#">m420040923_fts_sunset_r1.bal.ss</a> <a href="#">m420050920_fts_sunset_r1.bal.ss</a> <a href="#">m420070922_fts_sunset_r2.bal.ss</a> <a href="#">m420070923_fts_sunrise_r2.bal.ss</a> <a href="#">m420110923_fts_sunset_r1</a> <a href="#">m420110924_fts_sunrise_r1</a> <a href="#">m420140913_fts_sunset_r1</a> <a href="#">m420140914_fts_sunrise_r1</a>